Journal of Industrial and Engineering Chemistry 108 (2022) 484–492

Contents lists available at ScienceDirect

Journal of Industrial and Engineering Chemistry

journal homepage: www.elsevier.com/locate/jiec

Enhancement of the cycling stability of lithium-sulfur batteries by using a reactive additive for blocking dissolution of lithium polysulfides

Jun Hwan Ahn, Da-Ae Lim, Jiwan Kim, Tae-Sun You, Dong-Won Kim *

Department of Chemical Engineering, Hanyang University, Seoul 04763, South Korea

ARTICLE INFO

Article history:
Received 20 November 2021
Revised 2 January 2022
Accepted 19 January 2022
Available online 31 January 2022

Keywords:
Hexamethylene diisocyanate
Reactive additive
Lithium-sulfur battery
Lithium polysulfide
Electrochemistry

ABSTRACT

Hexamethylene diisocyanate was employed as a reactive additive to capture lithium polysulfides formed at the cathode of lithium-sulfur batteries. Unlike other solid additives used to trap polysulfides through physical and chemical interactions, it could effectively capture lithium polysulfides through chemical reaction between hexamethylene diisocyanate and lithium polysulfides at the electrode–electrolyte interface. A small amount of hexamethylene diisocyanate was enough to completely block the dissolution of lithium polysulfides into liquid electrolyte due to its high chemical reactivity, which enhanced the cycling stability of the lithium-sulfur battery while maintaining its high energy density. Our results demonstrate that the addition of hexamethylene diisocyanate to liquid electrolyte can provide an efficient strategy to address dissolution of lithium polysulfides and achieve good cycling stability in the high energy–density lithium-sulfur batteries.

Introduction

Emerging markets for personal and mobile electronic devices, unmanned aerial vehicles, long-range electric vehicles and grid-scale energy storage systems require high energy density lithium-ion batteries at lower costs [1–5]. To date, high energy densities and low costs have been primarily achieved through advanced manufacturing techniques and mass production, with little changes in battery materials or chemistry. The advent of cobalt-free cathodes is expected to help develop high energy density batteries and reduce costs. Extensive research on next-generation energy storage materials and systems has identified promising candidates, with lithium-sulfur batteries presenting the most encouraging results. The high theoretical capacity, non-toxicity, natural abundance and low price of sulfur make the lithium-sulfur battery an attractive option. However, due to the dissolution and migration of lithium polysulfides formed at the cathode during the discharge process, the lithium-sulfur battery that utilizes sulfur as a cathode active material suffers from rapid capacity fading [6–8]. Accordingly, much effort has been made to mitigate this problem, but initial approaches that physically block polysulfides by porous carbon matrix proved insufficient for prolonged cycles due to weak interactions between polysulfides and the carbon matrix. Further confinement of polysulfides was achieved by introducing polar host materials that trap polysulfides through electrostatic and chemical interactions [9–15]. However, chemical confinement could not trap all the polysulfides generated in the lithium-sulfur battery during cycling. Tests of state-of-the-art polysulfide host materials showed that even a highly conductive, polar and light host material with an exceptionally large surface area could confine polysulfides (Li_2S_4) corresponding to only 27 wt.% of the host material at best [16]. Considering that the amount of the host material is usually far less than that of sulfur in commercially viable lithium-sulfur batteries, this implies that host materials with a large surface area cannot trap all the polysulfides within a cathode without the assistance of other cell components. In this respect, modifying liquid electrolyte may be useful, however, few studies on liquid electrolyte in lithium-sulfur batteries have been conducted so far. Substituting conventional ether-based solvents with less-solvating solvents could lower the solubility of polysulfides, but resulted in poor dissolution of lithium salts [17–19]. Introducing gel polymer electrolyte to impede the dissolution and diffusion of polysulfides has be also attempted, but few polymer materials were chemically stable against highly reactive polysulfides, and previous studies mainly focused on physical gelation of entire electrolytes, which hindered favorable electrochemical reactions [20–22].

Instead of following the conventional approaches, here we suggest for the first time the use of hexamethylene diisocyanate (HDI)

* Corresponding author.
E-mail address: dongwonkim@hanyang.ac.kr (D.-W. Kim).

https://doi.org/10.1016/j.jiec.2022.01.025
1226-086X/

as a reactive additive to induce chemical reactions with lithium polysulfides formed on a cathode. Diisocyanates are known for their high reactivity with polyol compounds, including hydroxyl (–OH) groups, which are typically used to produce polyurethanes by step-growth polymerization. The carbon in the isocyanate (-N=C= O) is positively charged due to its low electronegativity and is therefore attacked by the negatively charged nucleophile oxygen in the hydroxy group. Hydrogen undergoes a nucleophilic addition reaction and adds to the negatively charged nitrogen in C=N bond. Diisocyanates adjacent to a benzene ring exhibit much higher reactivity than that of aliphatic diisocyanates, with HDI exhibiting the lowest reactivity among them. This supports the introduction of HDI to liquid electrolyte, as it does not react with any components except for the lithium polysulfides. Our results show that the addition of HDI results in chemical reaction with lithium polysulfides to form a polymeric layer at the electrolyte–electrode interface without external stimulation. This property is considered ideal for an electrolyte additive that locally confines polysulfides in lithium-sulfur batteries. Reactivity and diffusion tests were conducted to demonstrate the high reactivity of HDI with lithium polysulfides, and structure of the reaction product was investigated by Fourier-transform infrared (FT-IR), Raman, and X-ray photoelectron spectroscopy (XPS) analyses. An evaluation of the electrochemical performance of lithium-sulfur cells with liquid electrolyte containing optimum amount of HDI revealed that significant enhancement of cycling stability could be achieved, even in a cathode with high sulfur loading.

Experimental

Materials

Molecular sieves were immersed in HDI (Junsei Chemical), 1,3-dimethoxyethane (DME, Sigma Aldrich), 1,2-dioxolane (DOL, Sigma Aldrich) and tetra(ethylene glycol) diacrylate (TEGDA, Sigma Aldrich) for 24 h to remove trace amounts of water in the reagents. Sulfur powder (Sigma Aldrich) and polyethylene (PE) separator (ND420, Asahi Kasei) were vacuum dried at 60 ℃ for 12 h before use, and 2,2-azobisisobutyronitrile (AIBN, Junsei Chemical) was used as a thermal initiator. Liquid electrolyte was prepared by dissolving 1 M lithium bis(trifluoromethanesulfonyl) imide (LiTFSI, Panax Etec) and 0.4 M $LiNO_3$ (Sigma Aldrich) in a mixed solvent of DME/DOL (1:1 by volume) in an argon-filled glove box. A different amount of HDI (1, 3, 5 wt.%) was added to the liquid electrolyte to induce a chemical reaction with lithium polysulfide.

Synthesis of lithium polysulfide and reactivity study with HDI

Lithium polysulfide (Li_2S_8) was synthesized from sulfur powder and lithium metal (8:2 by molar ratio) in DME/DOL (1:1 by volume) solvent at 60 ℃ for 72 h, as reported earlier [23]. It was then diluted with DME/DOL to attain 10 wt.% Li_2S_8 solution for reactivity tests. Different amounts of HDI (1, 3, 5 wt.%) were added to DME/DOL (1:1 by volume) and each was mixed with the 10 wt.% Li_2S_8 solution. The mixed solution was kept at room temperature for 10 min. A gel precursor solution was prepared by mixing TEGDA and DME/DOL for 6 h. AIBN (1 wt.% of TEGDA) was added to the precursor solution, and the solution was thermally cured at 80 ℃ for 2 h.

Characterization and measurements

FT-IR spectroscopy was carried out between 400 and 4000 cm^{-1} using a Nicolet iS50 spectrometer. Raman spectra were obtained with a LabRAM HR Evolution Raman spectrometer (Horiba Scientific, 785 nm laser source). A VG Multilab ESCA system 220i was used for XPS investigation of the chemical structure of the reaction products. The binding energy was calibrated using the C1s peak at 284.6 eV as a reference. All the spectra were fitted with a Lorentzian-Gaussian peak fit function and Shirley-type background using the XPSPEAK41 software. The morphology of electrodes was examined by a Hitachi S-4800 field emission scanning electron microscope (FE-SEM).

Electrode preparation and cell assembly

A coating slurry consisting of Ketjen black (EC-600JD), Super-P, poly(vinylidene fluoride) (3:3:2 by weight) was homogeneously blended in N-methyl-2-pyrrolidone (NMP, Sigma Aldrich) with a planetary centrifugal mixer (Thinky Mixer, ARE-310). The resulting slurry was cast onto aluminum foil with a doctor blade to prepare the carbon electrode and vacuum dried under 80 °C for 12 h to remove residual NMP. A sulfur cathode with highly active material loading was then prepared by dropping 10 wt.% Li_2S_8 solution onto the carbon electrode in an argon-filled glove box and drying the electrode at 60 ℃ for 12 h in a vacuum oven. The loading level of Li_2S_8 in the cathode corresponded to the areal capacity of 5.6 mAh cm^{-2} based on sulfur chemistry (1 g sulfur = 1675 mAh). It should be noted that loading of conventional elemental sulfur did not reach a comparable value (5.6 mAh cm^{-2}) due to the inevitable formation of cracks upon high sulfur loading in the cathode. A lithium-sulfur cell (CR2032, coin-type) was assembled by sandwiching a PE separator between a lithium metal anode (200 μm, Honjo Metal Co. ltd.) and the abovementioned cathode, and injecting 80 μL of liquid electrolyte (with and without HDI) in an argon-filled glove box.

Electrochemical measurement

A PE separator covered with reaction product was soaked with liquid electrolyte and then sandwiched between two stainless steel electrodes for conductivity measurements. The ionic conductivity was measured by impedance analyzer (Zahner Electrik IM6) in the frequency range of 1 MHz to 1 Hz at AC amplitude of 10 mV. The following equation was used to calculate the ionic conductivity (σ):

$$\sigma = \frac{L}{RA}$$

where L is the thickness of the sample, R is the bulk resistance of the sample, and A is the electrode area. Linear-sweep voltammetry was performed in a potential range of 3.0 – 6.0 V vs Li/Li^+ at a scan rate of 1 mV s^{-1} using CHI 660 (CH Instruments Inc.) to evaluate the oxidative stability of the liquid electrolyte. The galvanostatic plating and stripping in the symmetric Li/electrolyte/Li cells was carried out in the voltage range of −1.0 – 1.0 V at 0.5 mA cm^{-2} for 10 h. A cycling test was performed using a battery cycler (WBS3000, WonA Tech) in the voltage range of 1.6–2.7 V at a constant current density of 0.5 mA cm^{-2}. Two pre-conditioning cycles to form the stable solid electrolyte interphase (SEI) on the lithium anode were conducted at 0.2 mA cm^{-2} prior to the cycling test. Specific capacity was calculated based on the mass of sulfur in the cathode. Electrochemical impedance spectroscopy of the lithium-sulfur cell was carried out using a Zahner Electrik IM6 impedance analyzer over a range of 1 mHz to 100 kHz at an amplitude of 5 mV.

Results and discussion

Figure 1 presents the reaction mechanism and structure of the reaction product between long-chain polysulfides (Li_2S_x,

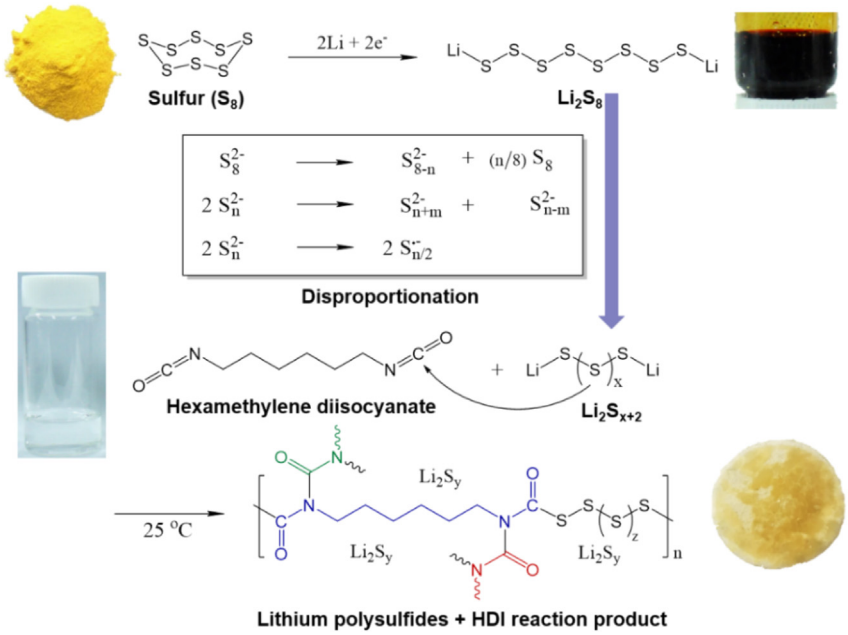

Fig. 1. Reaction mechanism between long-chain lithium polysulfides and hexamethylene diisocyanate (HDI).

$6 \leq x \leq 8$) and HDI. As the polysulfide anions (S_x^{2-}, $2 \leq x \leq 8$) have small differences in the Gibbs free energy of formation, sulfur chains can be easily transferred from one to another by disproportionation of the polysulfide anions. Due to constantly changing chain length and the generation of free radicals, various types of polysulfides can coexist in solution without external electron transfer. Polysulfide anions and radicals attack the partially positive carbons in the isocyanate (-N═C = O) group when mixed together, initiating a polymerization reaction. The partially negative nitrogen in the isocyanate group then attacks the adjacent carbon in another isocyanate, increasing the chain length of the polymer (propagation). To investigate the reactivity between HDI and lithium polysulfide, 5 mL solutions of different amounts of HDI (0, 1, 3 and 5 wt.%) were mixed with 10 wt.% Li_2S_8 solution (0.5 mL) in an argon-filled glove box at room temperature for 10 min. As shown in **Fig. S1a**, the lithium polysulfide solutions vigorously reacted with HDI. Even the solution containing 1 wt.% HDI produced a solid product within 10 min, indicating high reactivity between HDI and lithium polysulfide. For comparison purposes, DME/DOL solutions containing TEGDA (10 to 30 wt.%) and AIBN were kept at 80 ℃ for 2 h to induce radical polymerization. As presented in **Fig. S1b,** the 10 wt.% TEGDA solution did not form a polymer network sufficient to immobilize the DME/DOL solvent, implying lower reactivity of TEGDA compared with HDI in DME/DOL. These results confirm that HDI is highly reactive with polysulfide species, and can therefore be used as a reactive additive to suppress dissolution and migration of lithium polysulfides in a lithium-sulfur battery.

Figure S2 depicts a set of test kits designed to isolate two different solutions using a PE separator between them. The polysulfide solution was put into the small inner vial to leak through the porous PE membrane (porosity: 40 %). Large outer vials were then filled with different test solutions (0, 3 and 100 wt.% HDI) to compare the ability of HDI to suppress the diffusion of the lithium polysulfides. The test results are presented in Fig. 2. As shown in Fig. 2**a**, **a** large amount of lithium polysulfides in the small vial diffused through the PE membrane into the HDI-free DME/DOL solvent. After only 30 sec, the lithium polysulfides began to migrate to the DME/DOL solvent, resulting in little difference in the polysulfide concentration between the two solutions after 2 h. In contrast, the outer vial filled with pure HDI did not show any observable diffusion of the polysulfide species (Fig. 2**c**). HDI reacted vigorously with lithium polysulfide to form a solid product at the interface of two solutions, completely blocking the diffusion of lithium polysulfide to the outer vial. Product was formed only at the interface between the two solutions, and the rest of the solution remained intact. Due to its high reactivity, a small amount of HDI in DME/DOL solvent is expected to induce a chemical reaction between the HDI and lithium polysulfide. The solution containing 3 wt.% HDI also effectively blocked polysulfide diffusion through the PE membrane by forming a polymer layer at the interface (Fig. 2**b**). These results suggest that the addition of 3 wt.% HDI is sufficient to block dissolution and migration of lithium polysulfides in the DME/DOL-based liquid electrolyte. Photographs of a pristine PE separator and the resulting product formed on the PE separator are presented in **Fig. S3**. It can be clearly seen that yellowish polymer layer was produced on the PE separator, and it was confirmed that the product was not dissolved in the DME/DOL solvent. Since the polymer layer formed on the PE separator acts as a physical barrier or physical trap, the dissolution and migration of lithium polysulfides can be suppressed in the lithium-sulfur cell.

The chemical structure of reaction product was investigated in detail by FT-IR and Raman spectroscopy. According to the FT-IR spectra shown in Fig. 3**a**, HDI was characterized by a strong peak at 2252 cm^{-1}, which could be assigned to isocyanate (-N═C = O) groups. In the spectrum of the product between Li_2S_8 and HDI, the isocyanate peak completely disappeared, indicating the isocyanate groups in HDI reacted with lithium polysulfide. This is consistent with a previous report that the isocyanate peak vanished after polymerization [24–26]. Instead, new additional peaks corresponding to -C═O (1686 cm^{-1}) and -C—N (1528 cm^{-1}, 1136 cm^{-1}) were observed, which suggests the isocyanate groups in HDI reacted with lithium polysulfide to form a polymer chain [27,28]. The new peak at 1052 cm^{-1} could be assigned to the -S—C bonds, supporting a chemical reaction between HDI and polysulfide [29]. The formation of thiosulfate was confirmed by the peak at 1257 cm^{-1}, which was attributed to the chemical reaction between residual polysulfides and oxygen in the air [30]. Raman spec-

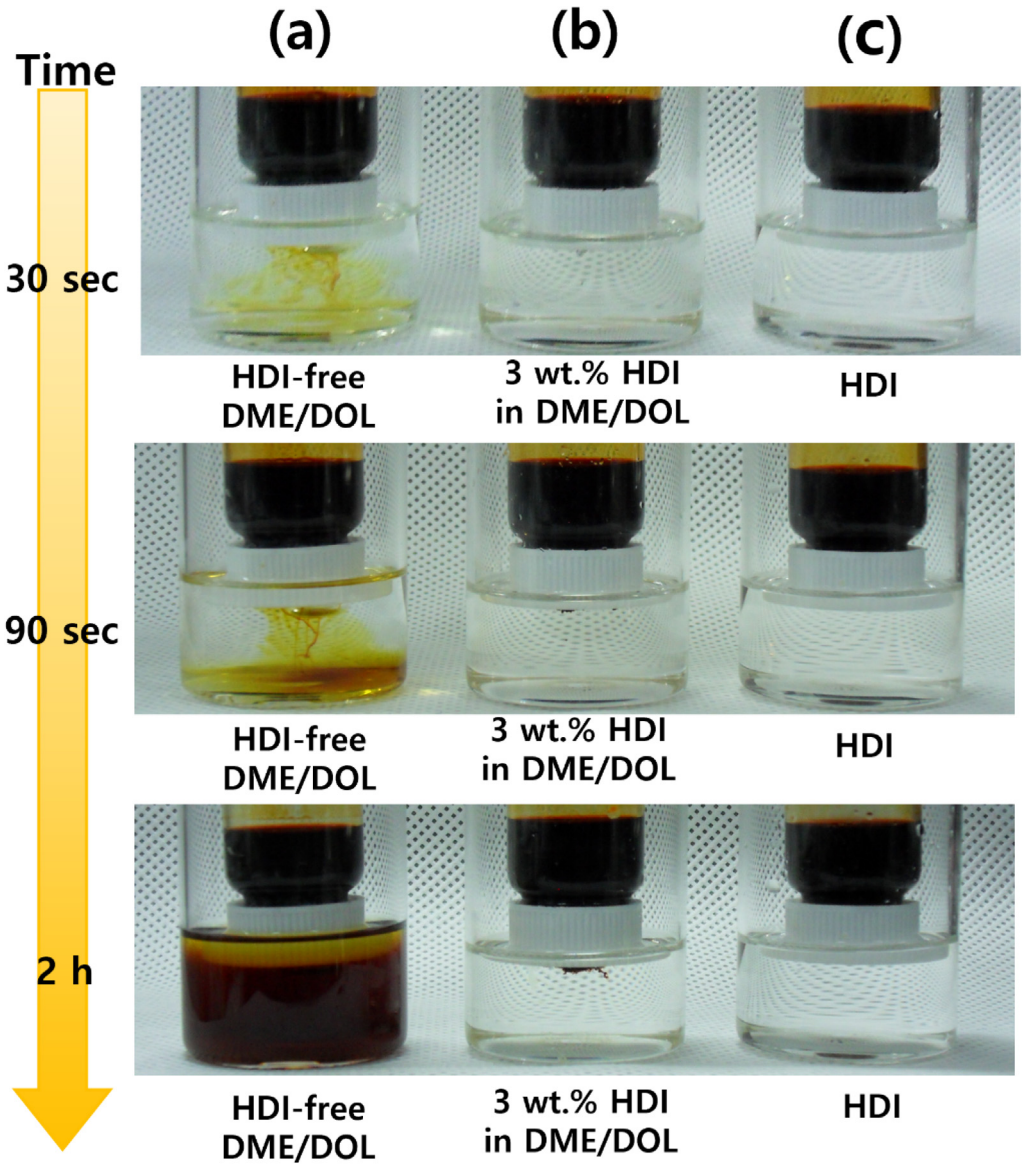

Fig. 2. Photographs for comparing the diffusion of lithium polysulfide through a porous PE separator to (a) HDI-free DME/DOL, (b) 3 wt.% HDI in DME/DOL and (c) pure HDI.

troscopy was also conducted to obtain structural information about the product, and the resulting spectra are shown in Fig. 3**b**. HDI did not show any intense peaks in the Raman spectrum below 600 cm^{-1}. Meanwhile, the Li_2S_8 dissolved in DME/DOL exhibited complex overlapping peaks from both non-ionic and ionic sulfurs of various chain lengths. As the allocation can vary depending on the experimental condition, the peaks in the Li_2S_8 solution and product can be explained by density functional theory calculation and experimental results reported previously [31–35]. Distinct peaks associated with long-chain sulfur S_8 were observed at 166.8, 233.0, 261.6, 452.8 and 486.9 cm^{-1}. Smaller peaks corresponding to shorter anionic polysulfides formed by disproportionation of the species also appeared in the Li_2S_8 solution. In the spectrum of the reaction product, the polysulfide exhibited an overall decrease in peak intensity. This result can be explained as follows. First, long-chain sulfurs reacted with HDI, and the chain length of the sulfur in the product may be shorter than S_8. Second, shorter anionic polysulfides, including species newly generated by not participating in the chemical reaction (i.e., split part from the long-chain) may be sufficiently reactive to form thiosulfates with oxygen from the air. This presumption could be confirmed by the relatively high intensity of peak at 430.1 cm^{-1}.

The structure of the reaction product was also investigated by XPS, and the overall survey spectrum is presented in Fig. 4**a**. Distinct peaks corresponding to C 1 s, N 1 s, O 1 s and S 2p were deconvoluted based on previous reports to identify the chemical structure of the product [36–43]. (Fig. 4**b-4e**) The C 1 s spectrum was resolved into four peaks centered at 284.6, 287.7, 289.0, and 292.9 eV, which can be assigned to C—C, newly formed C—S, C—N and -C═O bonds in the reacted isocyanate groups, respectively [36–38]. The N 1 s spectrum exhibited a single peak centered at 399.3 eV, which was attributed to C—N bonds in the reaction product [39]. The O 1 s spectrum showed two splitting peaks at 531.7 and 535.2 eV, which corresponded to thiosulfate and -C═O bonds, respectively [40,41]. The S 2p spectrum showed a spin–orbit coupling that split a single S 2p peak into S $2p_{3/2}$ and S $2p_{1/2}$ peaks (Δ = 1.16 eV, intensity ratio = 0.511). The C—S/S—S bonds at 164.9 eV and thiosulfate at 167.6 eV resulted from parasitic reactions between residual polysulfides and oxygen in the air, respectively [42,43]. Chemical analyses by FT-IR, Raman and XPS

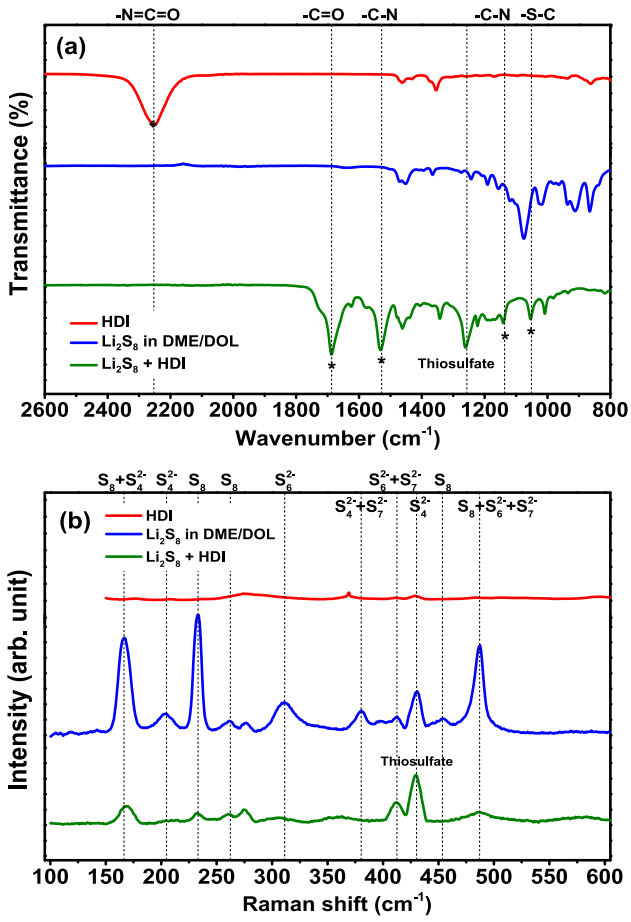

Fig. 3. (a) FT-IR and (b) Raman spectra of HDI, Li_2S_8 in DME/DOL and Li_2S_8 + HDI reaction products.

complemented each other, and based on these results, the reaction mechanism between lithium polysulfides and HDI suggests a molecular structure for the product, as previously discussed in Fig. 1.

When the lithium-sulfur cell is discharged, lithium polysulfides are formed on the cathode, and can react with HDI in the electrolyte based on previous results. In this case, the reaction products cover the entire surface of the cathode and block dissolution of the lithium polysulfides. To check whether lithium ions can transport through the product layer during cycling, we measured the ionic conductivity of a PE separator covered with the reaction product (**Fig. S3b**) after soaking it in the liquid electrolyte. The electrolyte was 1.0 M LiTFSI in DME/DOL containing 0.4 M $LiNO_3$. Product on the PE separator was swollen by liquid electrolyte and acted like a physical gel holding liquid electrolyte. Its ionic conductivity was measured to be 4.8×10^{-4} S cm^{-1}, indicating the facile conduction of lithium ions through the layer. It should be noted that the ionic conductivity of the pristine PE separator soaked with liquid electrolyte was 5.6×10^{-4} S cm^{-1}. The electrochemical stability the liquid electrolyte containing 3 wt.% HDI as an additive was investigated. In the linear sweep voltammograms of the reference liquid electrolyte and the electrolyte containing 3 wt.% HDI (**Fig. S4**), both electrolytes began to decompose rapidly near 4.5 V vs Li/Li$^+$. The liquid electrolyte containing 3 wt.% HDI showed no additional peaks below 4.5 V, demonstrating that its oxidative stability was sufficient to be applied to lithium-sulfur batteries. In order to investigate the effect of HDI on lithium metal, the galvanostatic plating and stripping cycling was performed in the symmetric Li/electrolyte/Li cells at 0.5 mA cm^{-2}. As shown in **Fig. S5**, the Li/electrolyte/Li cell with 3 wt.% HDI exhibited a higher overpotential than cell without HDI at early stage, which can be attributed high ionic resistance due to the addition of 3 wt.% HDI into the liquid electrolyte. However, its overpotential was gradually decreased and eventually stabilized. From these results, it is confirmed that the addition of HDI does not affect the cyclability of the Li plating/stripping reaction.

Based on the above results, it can be expected that HDI can serve as a reactive additive in the electrolyte to block dissolution and migration of lithium polysulfides in the lithium-sulfur cell. To control sulfur loading in the cathode, a precise amount of Li_2S_8 solution was dropped onto the carbon electrode. Thus, the cathode with a high areal capacity of 5.6 mAh cm^{-2} could be prepared, and its electrochemical performance was investigated using liquid electrolytes containing 1, 3, 5 wt.% HDI. Cycling performance of the lithium-sulfur cells was evaluated at a constant current density of 0.5 mA cm^{-2} after two pre-conditioning cycles at 0.2 mA cm^{-2}. **Fig. S6** depicts the voltage profiles of the cells assembled with liquid electrolytes containing different amounts of HDI at 0.5 mA cm^{-2}. As **Fig. S6** shows, 3 wt.% HDI was an optimum content for achieving the best cycling performance in terms of the discharge capacity and cycling stability. This is likely due to the fact that 1 wt.% HDI was not enough to capture all the lithium polysulfides, and 5 wt.% was too much, as HDI reacted with most of the lithium polysulfides necessary for reversible cycling. Fig. 5 compares the cycling performance of the lithium-sulfur cells employing liquid electrolytes with and without HDI (3 wt.%) at 0.5 mA cm^{-2}. Both cells exhibited an upper discharge plateau at 2.35 V and a lower discharge plateau at 2.10 V, which corresponded to the formation of long-chain polysulfides from the cyclic sulfur and the reduction of long-chain polysulfides to lithium sulfides (Li_2S), respectively. The cell using the HDI-containing electrolyte showed a longer second discharge plateau compared with the cell with the HDI-free liquid electrolyte. In the lithium-sulfur cells, the lithium polysulfides dissolved in the electrolyte can migrate to the anode side. The extended second discharge plateau in Fig. 5**a** indicates that more lithium polysulfides resided in the cathode without dissolution into the liquid electrolyte. As shown in Fig. 2**a**, the cell employing the liquid electrolyte without HDI did not block dissolution and migration of polysulfides, which implies that the lithium polysulfides in the liquid electrolyte, dissolved from the cathode, were not reutilized during subsequent reactions in the cell, resulting in reduced capacity at a lower discharge plateau. Discharge capacities of the two cells are compared as a function of the cycle number in Fig. 5**c**. In the cell with HDI-free electrolyte, a capacity loss during several tens of cycles arises from the dissolution of polysulfides into the liquid electrolyte. On the other hand, initial capacity loss in the cell employing HDI-containing electrolyte is caused by the chemical reaction of small amounts of polysulfides with HDI, until HDI is completely consumed by the reaction. It can be clearly seen that the cell assembled with the liquid electrolyte containing 3 wt.% HDI exhibited higher initial discharge capacity and superior capacity retention compared with those of the cell employing HDI-free liquid electrolyte. These results demonstrate that the cycling performance of the lithium-sulfur cell can be enhanced by adding small amounts of HDI into the liquid electrolyte, as the reaction product at the electrolyte–electrode interface efficiently blocks dissolution of lithium polysulfides during repeated cycling.

AC impedance of the lithium-sulfur cells was measured at fully charged state after two pre-conditioning cycles and the 200th cycle, respectively (Fig. 6). The x-axis intercept of the impedance spectrum corresponds to electrolyte resistance (R_e). Two semicircles appeared at high and medium to low-frequency regions are related to migration of lithium ions through the surface film on

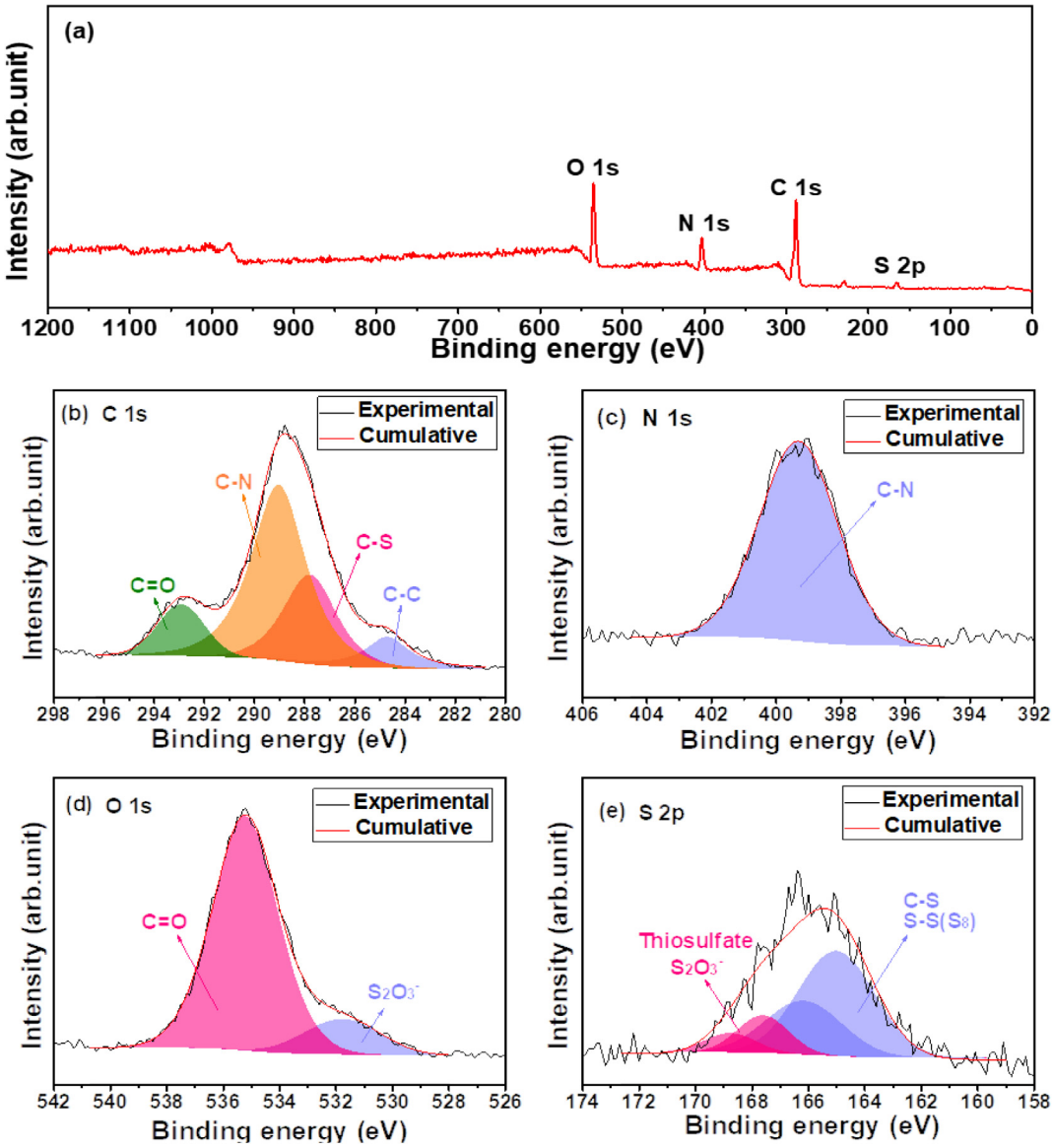

Fig. 4. XPS survey spectrum of the product and detailed spectra for specific elements. (a) Survey spectrum, (b) C 1 s, (c) N 1 s, (d) O 1 s and (e) S 2p.

the electrode (R_f) and the charge transfer process at the electrode–electrolyte interface (R_{CT}), respectively. Accordingly, the spectra could be fitted by using the equivalent circuit in Fig. 6**a** and the resulting resistance values are summarized in **Table S1**. As given in **Table S1**, two cells initially showed similar electrolyte resistance. Only the charge transfer resistance was observed to be slightly larger in the cell assembled with liquid electrolyte containing HDI, which was due to the product layer formed at the electrolyte–electrode interface by chemical reaction between HDI and lithium polysulfides during the pre-conditioning cycles. After 200 cycles, the two cells exhibited different spectra (Fig. 6**b**). The cell with HDI-free electrolyte gave rise to a large increase in both electrolyte resistance and overall interfacial resistances (R_f + R_{CT}) after 200 cycles. During repeated charge and discharge cycling of the cell, the lithium polysulfides dissolved in the liquid electrolyte causes an increase in the viscosity of electrolyte solution, which results in an increase in R_e. In addition, the formation of passivation layer (Li_2S) on lithium metal surface resulting from crossover of polysulfides mainly contributes to the increase of interfacial resistances. In contrast, the cell with the HDI-containing electrolyte showed a slight increase in electrolyte resistance (R_e) and film resistance (R_f) after 200 cycles. These results suggest that suppression of dissolution and migration of lithium polysulfides in the HDI-containing cell maintains the stable internal resistance of the cell and gives stable cycling behavior, compared with the cell employing HDI-free liquid electrolyte.

The morphology of the sulfur cathode was examined at fully charged state after 200 cycles. As presented in **Fig. S7b**, the cathode cycled in the liquid electrolyte without HDI exhibited an uneven and porous structure due to heterogeneous electrochemical reactions of the polysulfides and partial dissolution of lithium polysulfides during cycling, when compared with the pristine cathode before cycling (**Fig. S7a**). In contrast, the cathode cycled in the HDI-containing electrolyte was covered with a dense polymer layer (**Fig. S7c**). As revealed by XPS results in Fig. 7, the chemical structure of the surface layer on the cathode was almost consistent with the reaction product between HDI and lithium polysulfides. All the peaks from the reaction products were observed in the surface layer on the cathode, with small differences in the strong C—C bonds and new C-F bonds arising from the poly(vinylidene fluo-

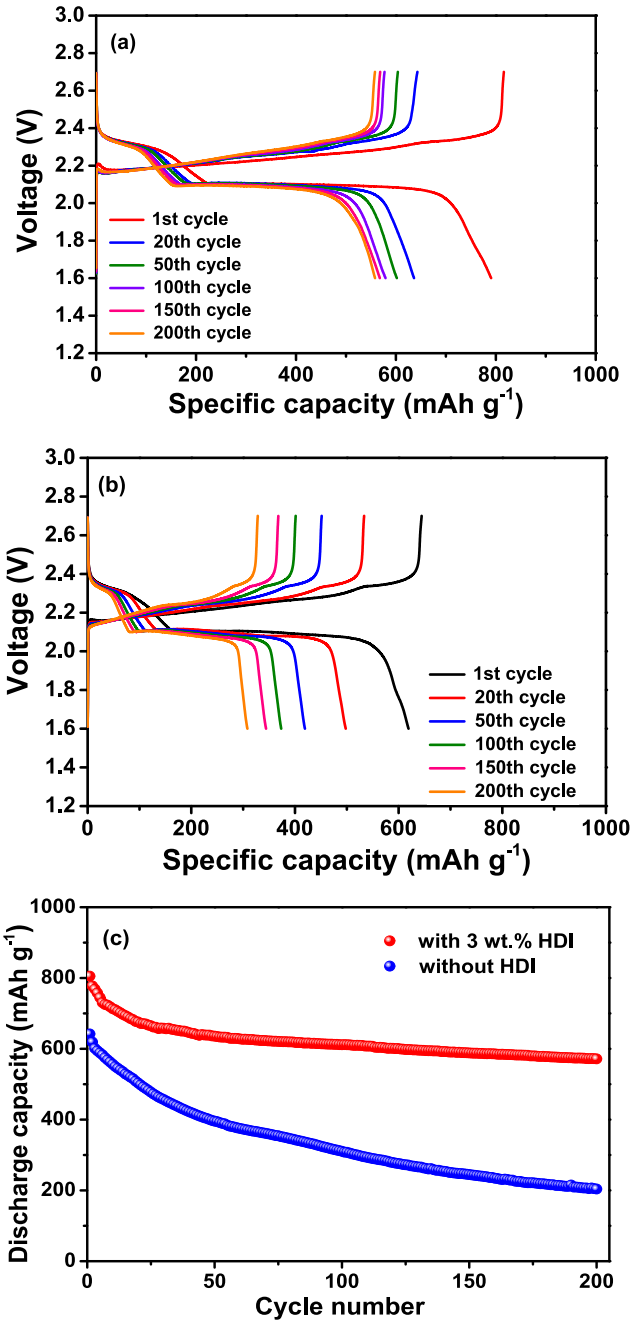

Fig. 5. Voltage profiles of the lithium-sulfur cells employing liquid electrolyte (a) with 3 wt.% HDI and (b) without HDI at 0.5 mA cm^{-2} and 25 ℃. (c) Discharge capacities of the cells with different electrolytes at 0.5 mA cm^{-2} and 25 ℃.

ride) binder in the cathode, indicating that the surface layer on the cathode was mainly formed by reactions between HDI and lithium polysulfides during cycling. It should be noted that peak positions in the high-resolution C1s spectrum (Fig. 7**a**) are changed compared to those in Fig. 4**b** except the C—C bond. Such a small peak shift in the C1s spectrum can be caused by charging effect of product due to its insulating nature [44,45]. Positive charge accumulates leading to so-called sample charging and shift of all core level peaks towards higher binding energy values, as the electrons leaving the surface are attracted by the positive potential. If electron charging is non-uniform, electrons in different regions of the product can experience different retarding potentials, which results in broadenings of the electronic peaks and even distortions.

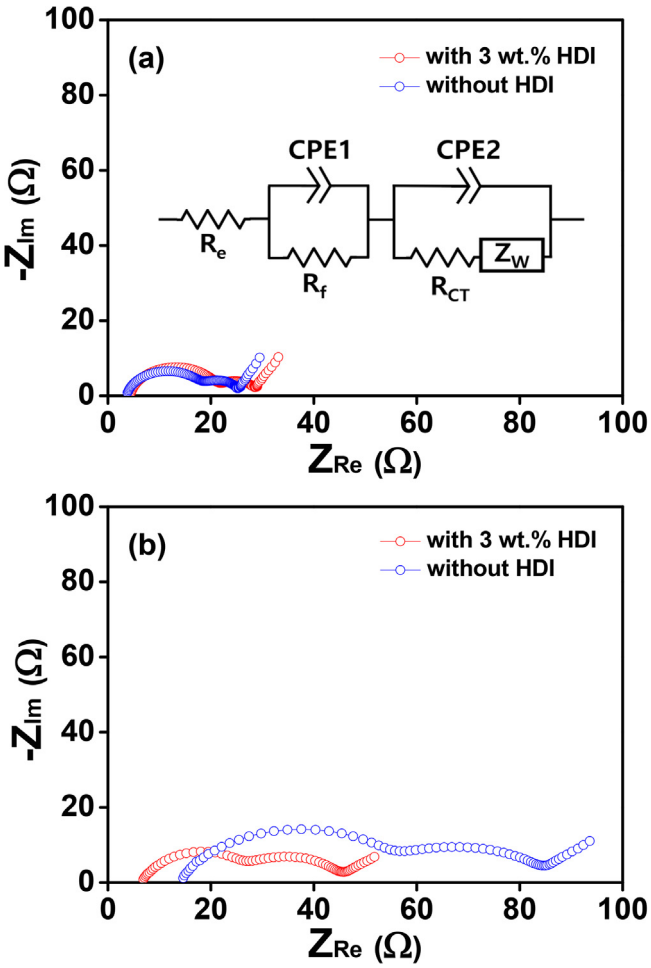

Fig. 6. AC impedance spectra of the lithium-sulfur cells with different electrolytes, which are obtained after (a) pre-conditioning cycles and (b) 200 cycles.

Although the product layer was responsible for large initial interfacial resistance (Fig. 6**a**) in the cell, it effectively suppressed dissolution and migration of polysulfides, resulting in good capacity retention even in the highly active mass-loaded lithium-sulfur cell (5.6 mAh cm^{-2}).

Conclusions

HDI was employed as a reactive and unprecedented additive to block dissolution of lithium polysulfides formed at the cathode in the lithium-sulfur battery. Chemical analyses based on FT-IR, Raman and XPS results confirmed that HDI reacted with lithium polysulfides to form the ion-conductive polymer layer at the interface. The lithium-sulfur batteries assembled with liquid electrolyte containing 3 wt.% HDI exhibited an initial discharge capacity of 805.3 mAh g^{-1} with a good capacity retention, despite highly active mass loading corresponding to the areal capacity of 5.6 mAh cm^{-2}. Our results indicate that the addition of small amount of HDI to liquid electrolyte can effectively block dissolution of lithium polysulfides and enhance the cycle life of high energy density lithium-sulfur batteries.

Declaration of Competing Interest

The authors declare that they have no known competing financial interests or personal relationships that could have appeared to influence the work reported in this paper.

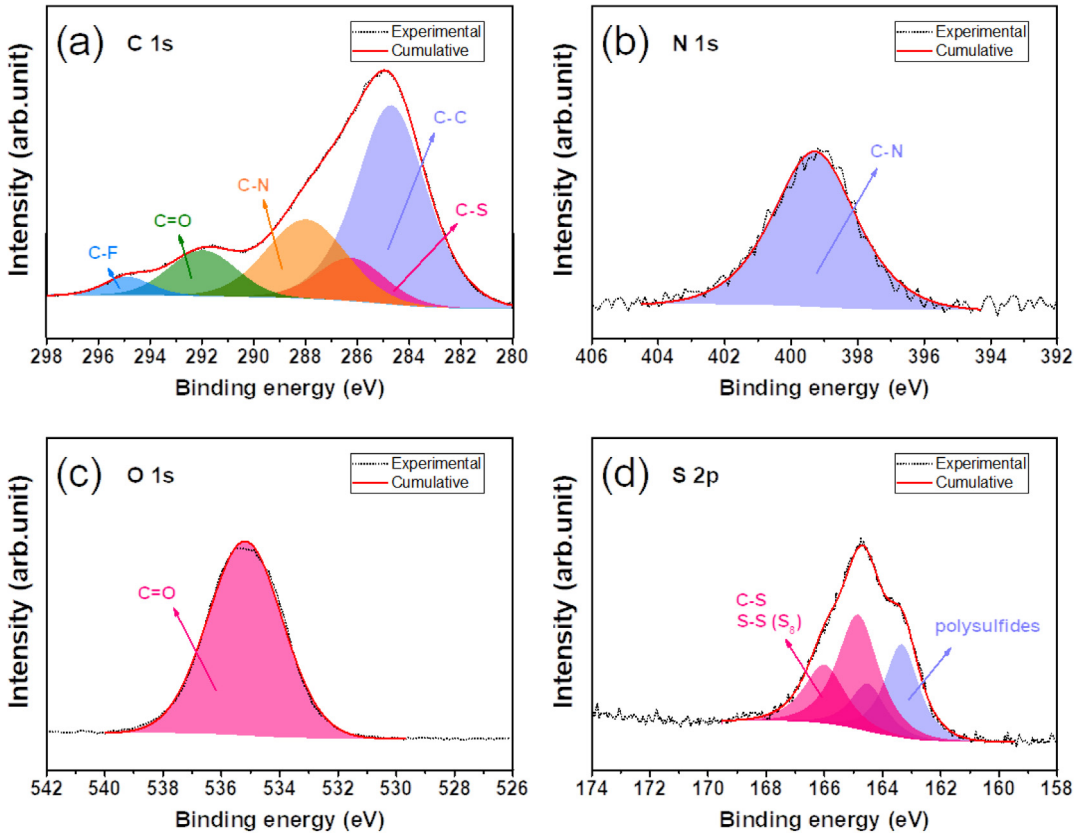

Fig. 7. XPS spectra of the surface layer formed on the cathode after 200 cycles. (a) C 1 s, (b) N 1 s, (c) O 1 s and (d) S 2p.

Acknowledgment

This work was supported by the National Research Foundation of Korea funded by the Korean Government (2019R1A4A2001527, 2021R1A2C2011050).

Appendix A. Supplementary data

Supplementary data to this article can be found online at https://doi.org/10.1016/j.jiec.2022.01.025.

References

[1] N. Nitta, F. Wu, J.T. Lee, G. Yushin, Mater. Today 18 (2015) 252–264, https://doi.org/10.1016/j.mattod.2014.10.040.
[2] M. Armand, J.M. Tarascon, Nature 451 (2008) 652–657, https://doi.org/10.1038/451652a.
[3] J.M. Tarascon, M. Armand, Nature 414 (2001) 359–367, https://doi.org/10.1038/35104644.
[4] V. Etacheri, R. Marom, R. Elazari, G. Salitra, D. Aurbach, Energy Environ. Sci. 4 (2011) 3243–3262, https://doi.org/10.1039/C1EE01598B.
[5] J.B. Goodenough, Y. Kim, Chem. Mater. 22 (2010) 587-603, 10.1021/cm901452z.
[6] P.G. Bruce, S.A. Freunberger, L.J. Hardwick, J.M. Tarascon, Nat. Mater. 11 (2012) 19–29, https://doi.org/10.1038/nmat3191.
[7] S. Evers, L.F. Nazar, Acc. Chem. Res. 46 (2013) 1135-1143, 10.1021/ar3001348.
[8] Y. Tang, Y. Huang, L. Luo, D. Fan, Y. Lu, A. Manthiram, Electrochim. Acta 367 (2021), https://doi.org/10.1016/j.electacta.2020.137482.
[9] H. Song, S. Suh, H. Park, D. Jang, J. Kim, H.-J. Kim, J. Ind. Eng. Chem. 99 (2021) 309–316, https://doi.org/10.1016/j.jiec.2021.04.033.
[10] R. Ponraj, A.G. Kannan, J.H. Ahn, D.-W. Kim, ACS Appl. Mater. Interfaces 8 (2016) 4000–4006, https://doi.org/10.1021/acsami.5b11327.
[11] R. Ponraj, A.G. Kannan, J.H. Ahn, J.H. Lee, J. Kang, B. Han, D.-W. Kim, ACS Appl. Mater. Interfaces 9 (2017) 38445–38454, https://doi.org/10.1021/acsami.7b10641.
[12] D.H. Lee, J.H. Ahn, M.S. Park, A. Eftekhari, D.-W. Kim, Electrochim. Acta 283 (2018) 1291–1299, https://doi.org/10.1016/j.electacta.2018.07.031.
[13] G.G. Kumar, S.H. Chung, T.R. Kumar, A. Manthiram, ACS Appl. Mater. Interfaces 10 (2018) 20627–20634, https://doi.org/10.1021/acsami.8b06054.
[14] S.-Y. Lee, Y. Choi, J.-K. Kim, S.-J. Lee, J.S. Bae, E.D. Jeong, J. Ind. Eng. Chem. 94 (2021) 272–281, https://doi.org/10.1016/j.jiec.2020.10.046.
[15] J.H. Ahn, G.K. Veerasubramani, S.M. Lee, T.S. You, D.-W. Kim, J. Electrochem. Soc. 166 (2019) A5201–A5209, https://doi.org/10.1149/2.0311903jes.
[16] Q. Pang, C.Y. Kwok, D. Kundu, X. Liang, L.F. Nazar, Joule 3 (2018) 136–148, https://doi.org/10.1016/j.joule.2018.09.024.
[17] M. Cuisinier, P.E. Cabelguen, B.D. Adams, A. Garsuch, M. Balasubramanian, L.F. Nazar, Energy Environ. Sci. 7 (2014) 2697–2705, https://doi.org/10.1039/C4EE00372A.
[18] K.A. See, H.L. Wu, K.C. Lau, M. Shin, L. Cheng, M. Balasubramanian, K.G. Gallagher, L.A. Curtiss, A.A. Gewirth, ACS Appl. Mater. Interfaces 8 (2016) 34360-34371, 10.1021/acsami.6b11358.
[19] C.W. Lee, Q. Pang, S. Ha, L. Cheng, S.D. Han, K.R. Zavadil, K.G. Gallagher, L.F. Nazar, M. Balasubramanian, ACS Cent. Sci. 3 (2017) 605-613, 10.1021/acscentsci.7b00123.
[20] M. Liu, D. Zhou, Y.B. He, Y. Fu, X. Qin, C. Miao, H. Du, B. Li, Q.H. Yang, Z. Lin, T.S. Zhao, F. Kang, Nano Energy 22 (2016) 278–289, https://doi.org/10.1016/j.nanoen. 2016.02.008.
[21] M. Liu, Y. Ren, D. Zhou, H. Jiang, F. Kang, T. Zhao, A.C.S. Appl, Mater. Interfaces 9 (2017) 2526–2534, https://doi.org/10.1021/acsami.6b14311.
[22] J.-W. Choi, J.-H. Kim, G. Cheruvally, J.-H. Ahn, K.-W. Kim, H.-J. Ahn, J.-U. Kim, J. Ind. Eng. Chem. 12 (2006) 939–949.
[23] M. Hagen, P. Schiffels, M. Hammer, S. Dorfler, J. Tubke, M.J. Hoffmann, H. Althues, S. Kaskel, J. Electrochem. Soc. 160 (2013) A1205-A1214, 10.1149/2.045308jes.
[24] A.K. Mishra, D.K. Chattopadhyay, B. Sreedhar, K.V.S.N. Raju, Prog. Org. Coat. 55 (2006) 231–243, https://doi.org/10.1016/j.porgcoat.2005.11.007.
[25] A.S. Nasar, G. Libni, RSC Adv. 7 (2017) 34149–34159, https://doi.org/10.1039/C7RA03734A.
[26] J. Ederer, P. Janos, P. Ecorchard, J. Tolasz, V. Stengl, H. Benes, M. Perchacz, O. Pop-Georgievski, RSC Adv. 7 (2017) 12464-12473, 10.1039/C6RA28745J.
[27] T.T. Calam, Electroanalysis 32 (2020) 149–158, https://doi.org/10.1002/elan.201900450.
[28] Y.C. Chen, W. Tai, Polymers 10 (2018) 1100–1111, https://doi.org/10.3390/polym10101100.
[29] A.A. Tsyganenko, F. Can, A. Travert, F. Mauge, Appl. Catal. A-Gen. 268 (2004) 189–197, https://doi.org/10.1016/j.apcata.2004.03.038.
[30] M. Smith, M. Bardiau, R. Brennan, H. Burgess, J. Caplin, S. Ray, T. Urios, NPJ Mater. Degrad. 3 (2019) 37, https://doi.org/10.5061/dryad.52vq8t5.

[31] H.L. Wu, M. Shin, Y.M. Liu, K.A. See, A.A. Gewirth, Nano Energy 32 (2017) 50–58, https://doi.org/10.1016/j.nanoen.2016.12.015.
[32] E.A. Nicol, J.Y. Baron, J. Mirza, J.J. Leitch, Y. Choi, J. Lipkowski, J. Solid State Electrochem. 18 (2014) 1469–1484, https://doi.org/10.1007/s10008-013-2320-z.
[33] Z. Lin, Z. Liu, W. Fu, N.J. Dudney, C. Liang, Angew. Chem. Int. Ed. 52 (2013) 7460–7463, https://doi.org/10.1002/anie.201300680.
[34] Q. Zou, Y.C. Lu, J. Phys. Chem. Lett. 7 (2016) 1518–1525, https://doi.org/10.1021/acs.jpclett. 6b00228.
[35] M. Cuisinier, C. Hart, M. Balasubramanian, A. Garsuch, L.F. Nazar, Adv. Energy Mater. 5 (2015) 1401801, https://doi.org/10.1002/aenm.201401801.
[36] P. Gobbo, Z. Mossman, A. Nazemi, A. Niaux, M. C. Biesinger, E. R. Gillies, M. S. Workentin, J. Mater. Chem. B 2 (2014) 1764-1769, 10.1039/C3TB21799J.
[37] Y. Jung, B. Kang, Phys. Chem. Chem. Phys. 18 (2016) 21500–21507, https://doi.org/10.1039/C6CP03146C.
[38] E. Markevich, G. Salitra, Y. Talyosef, F. Chesneau, D. Aurbach, J. Electrochem. Soc. 164 (2017) A6244–A6253, https://doi.org/10.1149/2.0391701jes.
[39] A. Mohtasebi, T. Chowdhury, L.H.H. Hsu, M.C. Biesinger, P. Kruse, J. Phys. Chem. C 120 (2016) 29248–29263, https://doi.org/10.1021/acs.jpcc.6b09950.
[40] T. Lei, Y. Xie, X. Wang, S. Miao, J. Xiong, C. Yan, Small 13 (2017) 1701013, https://doi.org/10.1002/smll.201701013.
[41] S. Wu, J. Wang, S. Song, D.H. Xia, Z. Zhang, Z. Gao, J. Wang, W. Jin, W. Hu, J. Electrochem. Soc. 164 (2017) C94–C103, https://doi.org/10.1149/2.0541704jes.
[42] X. Liang, C. Hart, Q. Pang, A. Garsuch, T. Weiss, F. Nazar, Nat. Commun. 6 (2015) 5682–5689, https://doi.org/10.1038/ncomms6682.
[43] H. Kim, J. Lee, H. Ahn, O. Kim, M. J. Park, Nat. Commun. 6 (2015) 7278, 10.1038/ncomms8278.
[44] J. Cazaux, J. Electron. Spectrosc. Relat. Phenom. 105 (1999) 155-185, 10.1016 / S0368-2048(99)00068-7.
[45] G. Greczynski, L. Hultman, Prog. Mater. Sci. 107 (2020) 100591, 10.1016/j.pmatsci.2019.100591.